

Inhibition Effect of Natural Junipers Extract towards Steel Corrosion in HCl Solution

L. Bammou¹, R. Salghi^{1,*}, A. Zarrouk², H. Zarrok³, S. S. Al-Deyab⁴, B. Hammouti^{2,4},
M. Zougagh⁵, M. Errami¹

¹Equipe de Génie de l'Environnement et de Biotechnologie, ENSA, Université Ibn Zohr, BP 1136

²LCAE-URAC18, Faculté des Sciences, Université Mohammed Premier, BP 4808, Oujda, Morocco.

³Laboratoire des procédés de séparation, Faculté des Sciences, Kénitra, Morocco

⁴Petrochemical Research Chair, Department of Chemistry - College of Science, King Saud University, B.O. 2455 Riaydh 11451 Saudi Arabia.

⁵Regional Institute for Applied Chemistry Research, IRICA, Ciudad Real, Spain

*E-mail: r_salghi@yahoo.fr

Received: 12 July 2012 / Accepted: 3 August 2012 / Published: 1 September 2012

The objective of this study was to determine the effect of junipers extract (JE) on the corrosion of C38 steel in 1M HCl solution. The corrosion rate and mechanism were determined with the use of Tafel slopes, mass loss method and electrochemical impedance spectroscopy (EIS). The results showed that the inhibition efficiency increases with the increase of junipers extract (JE) concentration. Potentiodynamic polarization curves indicated that junipers extract (JE) as mixed type inhibitor. The effect of temperature on the inhibition efficiency was studied. The semicircles tended to open at lower frequencies in the Nyquist plots which indicates the rupture of the protective film. The adsorption follows Langmuir adsorption isotherm.

Keywords: Polarisation, EIS, Corrosion inhibition, Steel, Junipers extract, Acid medium

1. INTRODUCTION

Steel and steel-based alloys of different grades steel are extensively used in numerous applications where acid solutions are widely applied such as industrial acid pickling, industrial acid cleaning and oil-well acidizing [1]. The use of chemical inhibitors is one of the most practical methods for the protection against corrosion in acidic media. Most of the excellent acid inhibitors are organic compounds containing nitrogen, oxygen, phosphorus and sulphur [2–12]. The use of non-toxic inhibitors called green or eco-friendly environmental inhibitors is one of the solutions possible to prevent the corrosion of the material. These advantages have incited us to draw a large part of program

of our laboratory to examine natural substances as corrosion inhibitors such as: *prickly pear seed oil* [13], *Argan oil* [14,15], *Argan extract* [15-17], *Fennel oil* [18], *Rosemary oil* [19-21], *Thymus oil* [22,23], *Lavender oil* [24], *Jojoba oil* [25], *Pennyroyal Mint oil* [26], *allylpulegols* [27] and *Artemisia* [28,29].

In the present work, we investigate the corrosion inhibition of steel in 1 M HCl by junipers extract using weight loss, potentiodynamic polarization and electrochemical impedance spectroscopy (EIS) methods.

2. MATERIALS AND METHODS

2.1. Weight loss measurements

Coupons were cut into $2 \times 2 \times 0.08 \text{ cm}^3$ dimensions having composition (0.179% C, 0.165% Si, 0.439% Mn, 0.203% Cu, 0.034% S and Fe balance) are used for weight loss measurements. Prior to all measurements, the exposed area was mechanically abraded with 180, 320, 800, 1200 grades of emery papers. The specimens are washed thoroughly with bidistilled water, degreased and dried with ethanol. Gravimetric measurements are carried out in a double walled glass cell equipped with a thermostated cooling condenser. The solution volume is 80 cm^3 . The immersion time for the weight loss is 6 h at 298 K.

2.2. Electrochemical tests

The electrochemical study was carried out using a potentiostat PGZ100 piloted by Voltmaster software. This potentiostat is connected to a cell with three electrode thermostats with double wall (Tacussel Standard CEC/TH). A saturated calomel electrode (SCE) and platinum electrode were used as reference and auxiliary electrodes, respectively. The material used for constructing the working electrode was the same used for gravimetric measurements. The surface area exposed to the electrolyte is 0.094 cm^2 .

Potentiodynamic polarization curves were plotted at a polarization scan rate of 0.5 mV/s . Before all experiments, the potential was stabilized at free potential during 30 min. The polarisation curves are obtained from -800 mV to -400 mV at 298 K. The solution test is there after de-aerated by bubbling nitrogen. Gas bubbling is maintained prior and through the experiments. In order to investigate the effects of temperature and immersion time on the inhibitor performance, some test were carried out in a temperature range 298–328 K.

The electrochemical impedance spectroscopy (EIS) measurements are carried out with the electrochemical system (Tacussel), which included a digital potentiostat model Voltalab PGZ100 computer at E_{corr} after immersion in solution without bubbling. After the determination of steady-state current at a corrosion potential, sine wave voltage (10 mV) peak to peak, at frequencies between 100 kHz and 10 mHz are superimposed on the rest potential. Computer programs automatically controlled the measurements performed at rest potentials after 0.5 hour of exposure at 298 K. The impedance

diagrams are given in the Nyquist representation. Experiments are repeated three times to ensure the reproducibility.

2.3. Solutions preparation

Sample of *juniperus* plant was collected from the area of Midelt (located in Morocco) at July month 2011. Dried and pulping plant were crushed. Stock solution of the extract was prepared by stirring cold weighed amounts of the juniperus plant for 24 h in 1 M HCl solution (The solution 1M HCl was prepared by dilution of analytical grade 37% HCl with double distilled water). The resulting solution was filtered. This extract was used to study the corrosion inhibition properties and to prepare the required concentrations. The solution tests are freshly prepared before each experiment.

3. RESULTS AND DISCUSSION

3.1. Gravimetric measurements

3.1.1. Effect of concentration

Weight loss experiments were done according to the method described previously [30]. All the tests were conducted in aerated 1 M HCl at 298 K with different concentrations of junipers extract (JE). At the end of the tests the specimen were carefully washed in acetone and then weighed. Duplicate experiments were performed in each and the mean value of the weight loss has been reported. The inhibition efficiency (E_w %) and surface coverage (Θ) were determined by using the following equations:

$$E_w \% = \left(1 - \frac{W_{corr}}{W_{corr}^0} \right) \times 100 \quad (1)$$

$$\Theta = 1 - \frac{W_{corr}}{W_{corr}^0} \quad (2)$$

Where W_{corr} and W_{corr}^0 are the weight losses for C38 steel in the presence and absence of the extract in HCl solution and Θ is the degree of surface coverage of the inhibitor.

Percentage inhibition efficiency, corrosion rate and surface coverage in 1M hydrochloric acid with different concentration of this extract are given in Table 1. It can be seen from the table that the inhibition efficiency of the inhibitor increases with increasing concentration of inhibitor. The variation of percentage inhibition efficiency (E_w %) and corrosion rate with inhibitor concentration is depicted graphically in Fig. 1 for 1M hydrochloric acid. Percentage inhibition efficiency (E_w %) with the concentration of inhibitor, indicate that the inhibition efficiency increases with increasing inhibitor concentration. From Table 1 it is observed that the corrosion rate decreases with increasing concentration of inhibitor. The surface coverage increases with increasing the concentration of inhibitor.

Table 1. Corrosion rate of steel in 1M HCl with and without junipers extract various concentrations, and the corresponding inhibition efficiency.

Inhibitor	Conc (g / L)	W_{corr} (mg/cm ² .h)	E_w (%)	Θ
Blank	0.0	1.2614	-	-
Junipers extract	4.0	0.6976	44.7	0.447
	5.0	0.4402	65.1	0.651
	6.0	0.1602	87.3	0.873

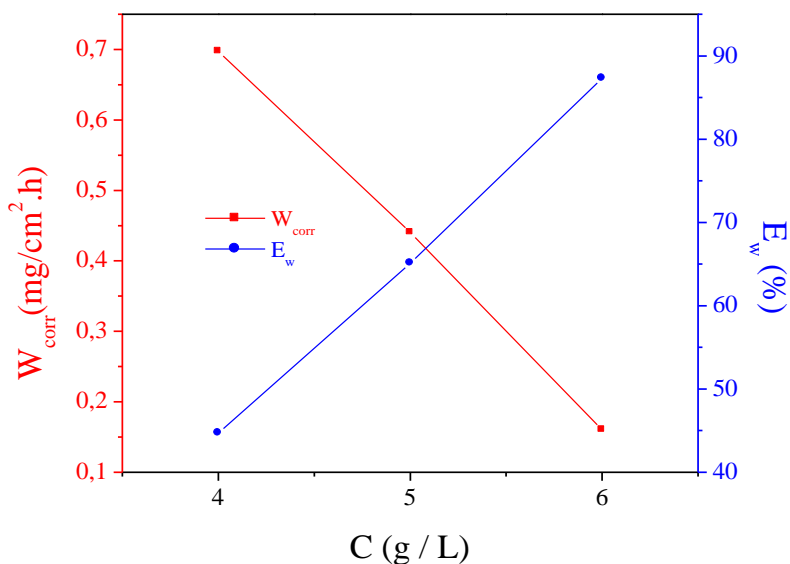


Figure 1. Variation of the corrosion rate and inhibitive efficiency against the extract concentrations.

3.1.2.Effect of temperature

Table 2. Various corrosion parameters for C38 steel in 1M HCl in absence and presence of optimum concentration of extract at different temperatures.

Temperature (K)	Inhibitor	W_{corr} (mg/cm ² .h)	E_w (%)	Θ
298	Blank	1.2614	-	-
	JE	0.1602	87.3	0.873
308	Blank	2.2354	-	-
	JE	0.5411	75.8	70.58
318	Blank	3.1022	-	-
	JE	1.0207	67.1	0.671
328	Blank	5.1215	-	-
	JE	2.2381	56.3	0.563

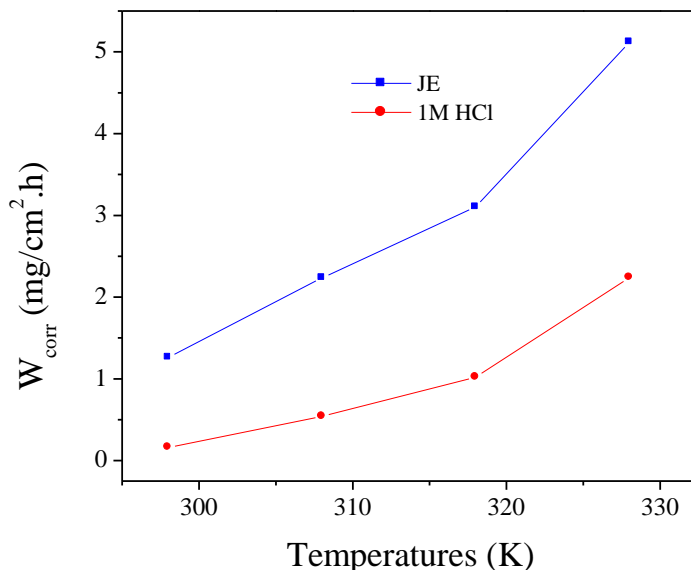


Figure 2. Variation of corrosion rate in 1M HCl on steel surface without and with of optimum concentration of extract at different temperatures

Temperature has great effect on the corrosion phenomenon. In general, the corrosion rate increases with rise in temperature. In this study, the effect of temperature on the corrosion and inhibition process of C38 steel in 1 M HCl in the absence and presence of optimum concentration of junipers extract after 1 h of immersion was followed at 298-328K using weight loss measurements. The result of the effect of temperature on corrosion rate as presented in Table 2 is in agreement with earlier reports [31–33] increasing as temperature increases. Fig. 2 illustrates the variation of corrosion rate in the absence and of inhibitor at optimum concentration at different temperatures.

The dependence of corrosion rate on temperature can be expressed by the Arrhenius equation [34]:

$$W_{corr} = A \exp\left(\frac{-E_a}{RT}\right) \tag{3}$$

where W_{corr} is the corrosion rate, E_a is the apparent activation energy of the C38 steel dissolution, R is the molar gas constant, T is the absolute temperature, and A is the frequency factor. Fig. 3 depicts Arrhenius plot as $\ln W_{corr}$ against the reciprocal of temperature ($1/T$) for C38 steel in 1 M HCl in the free acid solution and the acid containing different concentrations of junipers extract (JE). The plots obtained are straight lines and the activation energy was evaluated from the slope of the straight line plots. The calculated values of activation energy are listed in Table 3. It can be seen in the table that E_a is higher in the presence of the inhibitor than in the absence of the inhibitor. This observation further supports the proposed physical adsorption mechanism.

Table 3. Activation parameters for the steel dissolution in 1M HCl in the absence and the presence of JE at optimum concentration.

Inhibitor	A (mg/cm ² h)	Linear regression coefficient (r)	E _a (kJ/mol)	ΔH _a [*] (kJ/mol)	ΔS _a [*] (J/mol.K)
Blank	3.7062×10 ⁹	0.99581	36.84	34.24	-127.87
Junpers extract	2.8812×10 ¹¹	0.99293	69.63	67.03	-34.24

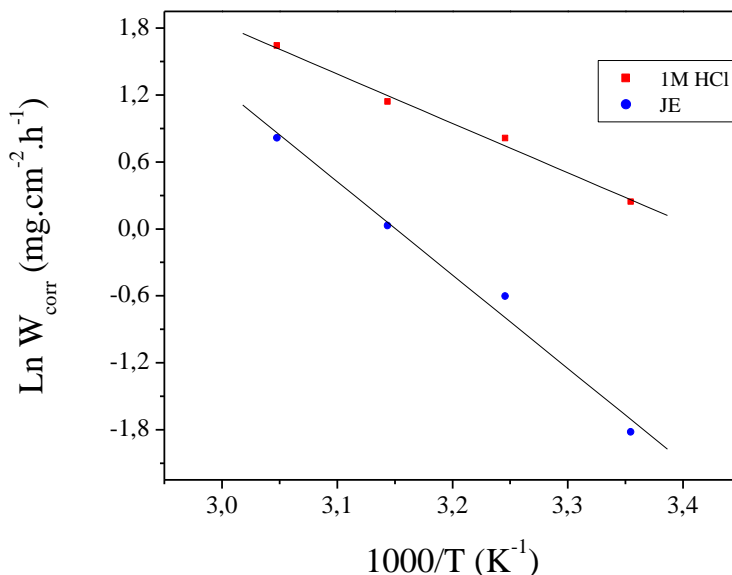


Figure 3. Arrhenius plots of Ln W_{corr}/T vs. 1/T for steel in 1M HCl in the absence and the presence of JE at optimum concentration.

Further insight into the adsorption mechanism is offered by considering the thermodynamic functions for the C38 steel dissolution in 1 M HCl in the absence and presence of optimum concentration of junipers extract (Fig. 4). In this regards, Transition state equation was used to evaluate the corrosion activation parameters, namely, the enthalpy of activation (ΔH_a^{*}) and entropy of activation (ΔS_a^{*}). Transition state equation is given by the expression:³⁴

$$W_{corr} = \frac{RT}{Nh} \exp\left(\frac{\Delta S_a^*}{R}\right) \exp\left(-\frac{\Delta H_a^*}{RT}\right) \tag{4}$$

Where W_{corr} is the corrosion rate, R the gas constant, T the absolute temperature, A the pre-exponential factor, h the Plank's constant and N is Avogadro's number, ΔH_a^{*} the enthalpy of activation and ΔS_a^{*} the entropy of activation.

Fig. 4 showed a plot of Ln (C_R/T) versus 1/T. The straight lines are obtained with a slope (ΔH_a^{*}/R) and an intercept of (Ln R/Nh + ΔS_a^{*}/R) from which the values of the values of ΔH_a^{*} and ΔS_a^{*} are

calculated and are given in Table 3. Inspection of these data revealed that the thermodynamic parameter (ΔH_a^*) for dissolution reaction of steel in 1 M HCl in the presence of extract is higher (67.03 KJ mol⁻¹) than that of in the absence of inhibitor (34.24 KJ mol⁻¹). The positive sign of ΔH_a^* reflect the endothermic nature of the steel dissolution process suggesting that the dissolution of steel is slow [35] in the presence of inhibitor.

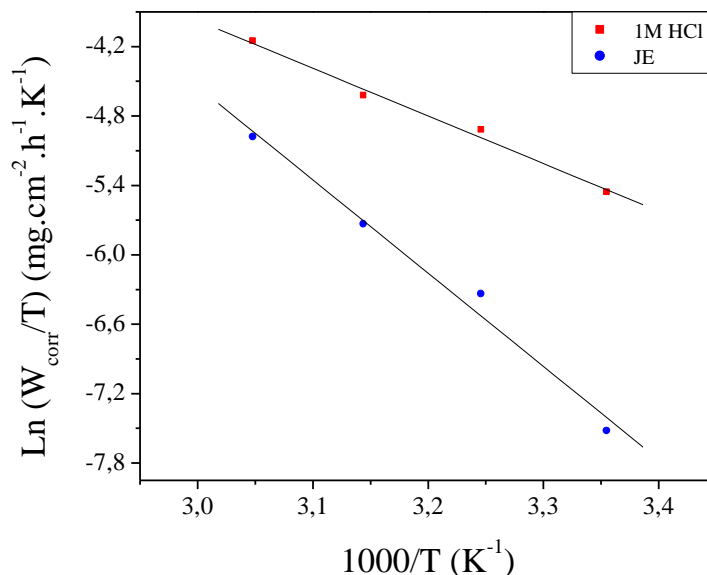


Figure 4. Arrhenius plots of $\text{Ln } W_{\text{corr}}/T$ vs. $1/T$ for steel in 1M HCl in the absence and the presence of JE at optimum concentration.

Large and negative value of entropic (ΔS_a^*) imply that the activated complex in the rate determining step represents an association rather than a dissociation step, meaning that a decrease in disordering takes place on going from reactant to the activated complex [36, 37].

3.1.3. Adsorption isotherm

Adsorption isotherms are usually used to describe the adsorption process. The most frequently used isotherm include: Langmuir, Frumkin, Hill de Boer, Parsons, Temkin, Flory-Huggins, Dhar-Flory-Huggins, Bockris-Swinkels and recently formulated thermodynamic / kinetic model of El Awady et al [38-40]. The establishment of adsorption isotherm that describes the adsorption of a corrosion inhibitor can provide important clues to the nature of the metal-inhibitor interaction. Adsorption of the organic molecules occurs as the interaction energy between the molecules and the metal surface is higher than between the H₂O molecule and the metal surface.⁴¹ In order to obtain the adsorption isotherm, the degree of surface coverage (Θ (Eq.2)) for the various concentrations of the inhibitor has been calculated according to the formula. Langmuir isotherm was tested for its suitability to the experimental data. Langmuir isotherm is given as

$$\frac{\Theta}{1-\Theta} = K_{ads} C_{inh} \tag{5}$$

The rearrangement gives the following equation: $\frac{C_{inh}}{\Theta} = \frac{1}{K_{ads}} + C_{inh}$ (6)

Plot $\text{Log}(\Theta/1-\Theta)$ versus $\text{Log}(C)$ yield a straight line (Fig. 5) with regression coefficient, R^2 , almost equal to 1. This suggests that extract in present study obeyed the Langmuir isotherm and there is negligible interaction between the adsorbed molecules.

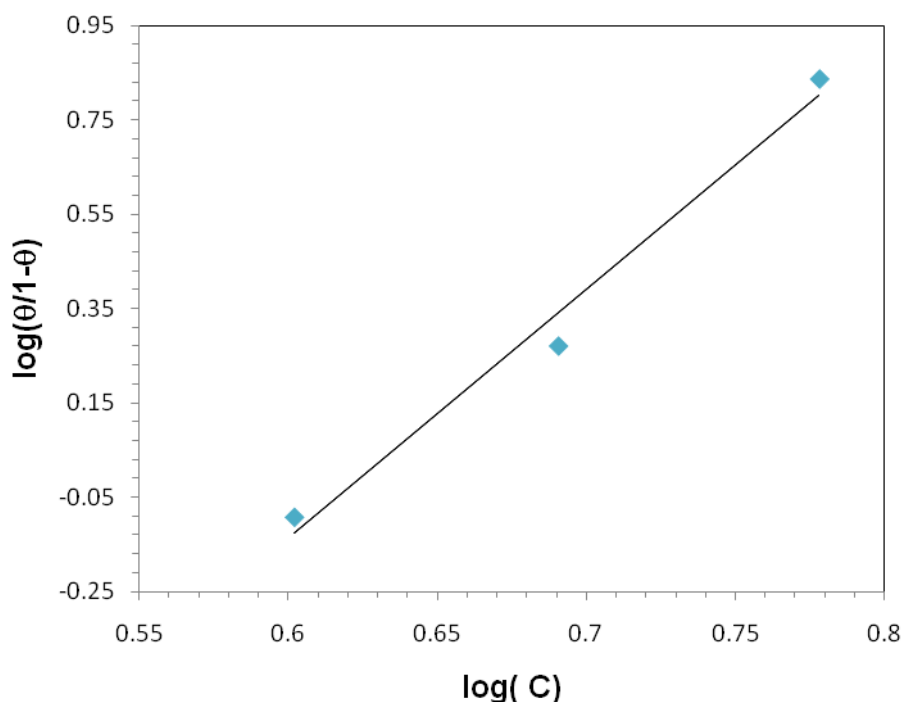


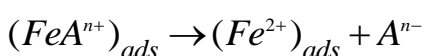
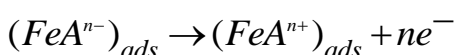
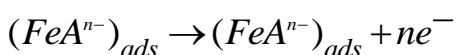
Figure. 5. Langmuir adsorption isotherm of junipers extract on the steel surface.

3.2. Polarization measurements

Polarisation measurements have been carried out in order to gain knowledge concerning the kinetics of the anodic and cathodic reactions. Polarisation curves of the C38 steel in 1 M HCl solutions without and with addition of different concentrations of junipers extract (JE) are shown in Fig. 6. The anodic and cathodic current–potential curves are extrapolated up to their intersection at a point where corrosion current density (I_{corr}) and corrosion potential (E_{corr}) are obtained [42]. Table 4 shows the electrochemical parameters (I_{corr} , E_{corr} , and b_c) obtained from Tafel plots for the steel electrode in 1 M HCl solution without and with different concentrations of the investigated junipers extract (JE). The I_{corr} values were used to calculate the inhibition efficiency, E_I (%) (listed in Table 4), using the following equation [43]:

$$E_I(\%) = \left(\frac{I_{corr} - I'_{corr}}{I_{corr}} \right) \times 100 \tag{7}$$

Where I_{corr} and I'_{corr} are uninhibited and inhibited corrosion current densities, respectively. Under the experimental conditions performed, the cathodic branch represents the hydrogen evolution reaction, while the anodic branch represents the iron dissolution reaction. They are determined by extrapolation of Tafel lines to the respective corrosion potentials. Some of the authors proposed the following mechanism for the corrosion of iron and steel in acid solution [44–46]:



The cathodic hydrogen evolution

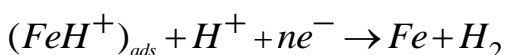
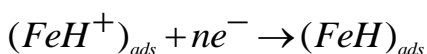
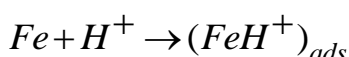


Table 4. Electrochemical parameters of steel in 1M HCl solution without and with junipers extract at different concentrations.

Inhibitor	Conc (g/L)	E_{corr} (mV/SCE)	I_{corr} ($\mu A/cm^2$)	$-b_c$ (mV/dec)	E_I (%)
Blank	0.0	-612	124	149	-
Junipers Extract	4.0	-600	72	164	41.9
	5.0	-588	43	170	65.3
	6.0	-601	12	113	90.3

It is shown from Fig. 6 that increasing the JE concentration reduces both the cathodic and the anodic currents, and there is no definite trend in the shift of E_{corr} values. Moreover, the recorded polarisation curves in the presence of inhibitor are characterized by the presence of anodic breakdown potential, E_b . The noble shift of E_b and the decrease of the corresponding current densities with

increasing the inhibitor concentration reflect the formation of anodic protective film on the electrode surface.⁴⁷ Based on the marked decrease of the cathodic and anodic current densities upon introducing the inhibitor in the aggressive solution, JE can be considered as a mixed-type inhibitor, meaning that the addition of JE reduces the anodic dissolution and also retards the cathodic hydrogen evolution reaction. In addition, the parallel cathodic Tafel curves in Fig. 6 show that the hydrogen evolution is activation controlled and the reduction mechanism is not affected by the presence of the inhibitor [48]. According to the anodic polarisation curves of JE in Fig. 6, it seems that the inhibitor did not show a corrosion inhibition effect at C38 steel electrode for the potential values higher than -300 mV/SCE. This potential can be defined as the desorption potential [49]. This phenomenon may be the result of significant steel dissolution, leading to desorption of the adsorbed film of the junipers extract inhibitor from the electrode surface.

The inspection of results in Table 3 indicate that JE inhibits the corrosion process in the studied range of concentrations and E (%) increases with C_{inh} , reaching its maximum value, 90.3%, at 6 g/L. The values of the cathodic Tafel lines, b_c , show slight changes with the addition of JE. This result means that the mechanism at the electrode reactions is not changed [49].

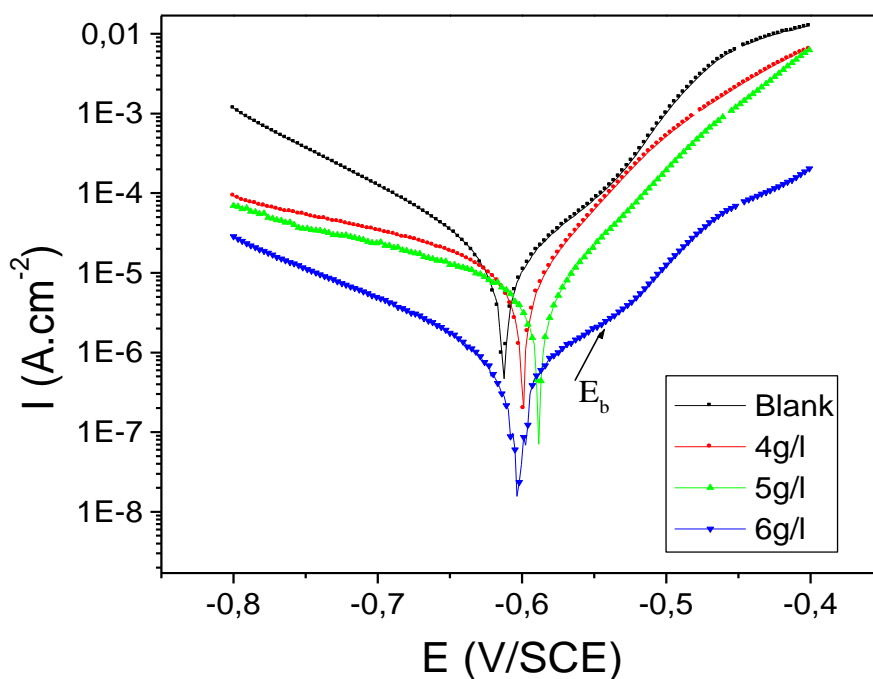


Figure 6. Potentiodynamic polarisation curves of steel in 1M HCl in the presence of different concentration of junipers extract.

3.3. Electrochemical impedance spectroscopy measurements

The corrosion behaviour of steel in 1M HCl solution, in the absence and presence of JE, is also investigated by the EIS at 298 K after 30 min of immersion. The charge-transfer resistance (R_{ct}) values are calculated from the difference in impedance at lower and higher frequencies, as suggested by Tsuru

et al [50]. The double layer capacitance (C_{dl}) and the frequency at which the imaginary component of the impedance is maximal ($-Z_{max}$) are found as represented in equation:

$$C_{dl} = \left(\frac{1}{\omega R_t} \right) \quad \text{where } \omega = 2\pi f_{max} \tag{8}$$

The inhibition efficiency got from the charge transfer resistance is calculated by:

$$E_{R_t} \% = \frac{R_{t(inh)} - R_t}{R_{t(inh)}} \times 100 \tag{9}$$

Where $R_{t(inh)}$ and R_t are the charge transfer resistance in the presence and absence of JE, respectively.

Fig.7 illustrate the electrochemical impedance diagrams for C-steel in a 1M HCl solution in the absence and presence of junipers extract (JE). Table 5 summarises the impedance data from EIS experiments carried out in both the absence and the presence of increasing extract concentrations. In extract-free solutions, only one depressed capacitive loop was observed and that loop can be attributed to the time constant of the charge transfer and the double layer capacitance. Such a depression is characteristic of solid electrodes and is often ascribed to dispersion effects, which have been attributed to roughness and inhomogeneities on the surface during corrosion [51, 52]. This behaviour is unaffected by the presence of the inhibitor, indicating the activation-controlled nature of the reaction during a onecharge transfer process.

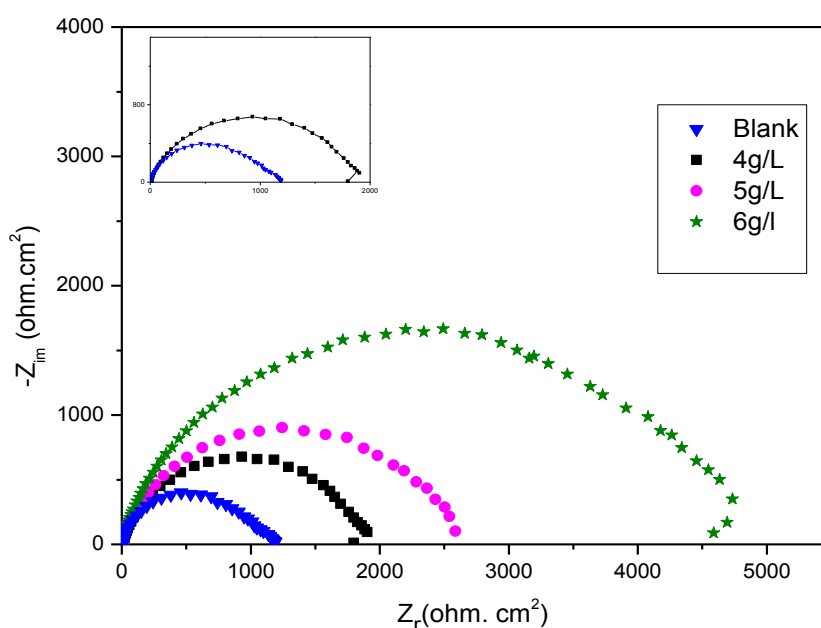


Figure. 7. Electrochemical impedance diagrams for C-steel in a 1M HCl solution in the absence and presence of junipers extract (JE).

Table 5. Impedance parameters for corrosion of steel in 1 M HCl in the absence and presence of different concentrations of junipers extract at 298 K.

Inhibitor	C (g/L)	R _{ct} (Ω.cm ²)	f _{max} (Hz)	C _{dl} (μF/cm ²)	E _{Rct} (%)
Blank	0.0	10	50	318	-
Junipers extract	4.0	19	12	698	47.4
	5.0	28	20	295	64.9
	6.0	82	62	31	87.8

A C_{dl} value of 318 nF/cm² was determined for the C-steel electrode in 1M HCl. The electrochemical impedance diagrams obtained in the presence of the extract also show only one depressed capacitive loop. Based on Table 5, it is clear that the R_{ct} values increased and the C_{dl} values decreased with increasing inhibitor concentration. These results may be attributable to the adsorption of the components in the junipers extract onto the metal/solution interface. Indeed, this hypothesis is corroborated by the anodic and cathodic polarisation curves and the corrosion potential results. A comparison of the inhibition efficiencies obtained using different methods (weight loss, polarisation curves and EIS methods). Fig. 8 shows a curve that compares the E (%) values obtained. One can see that whatever the method used, no significant changes are observed in E (%) values. We can then conclude that there is a good correlation with the three methods used in this investigation at all tested concentrations and that junipers extract (JE) is an efficient corrosion inhibitor.

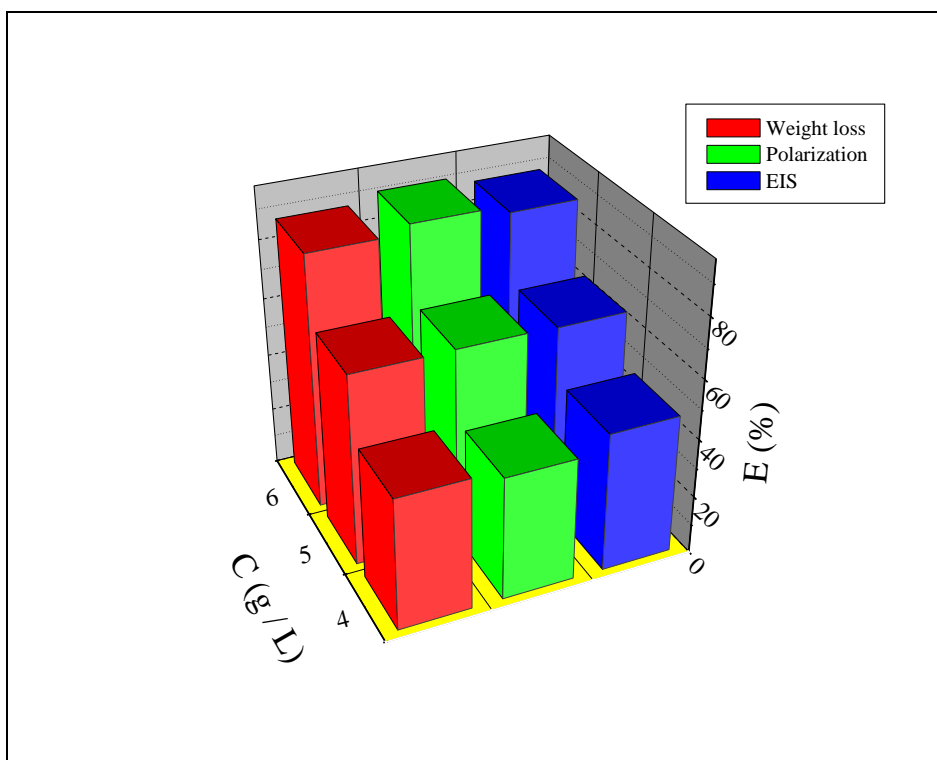


Figure. 8 . Comparison of inhibition efficiency (E %) values obtained by weight loss,polarisation and EIS methods.

4. CONCLUSION

The studied junipers extract (JE) shows excellent inhibition properties for the corrosion of C38 steel in 1M HCl at 298K, and the inhibition efficiency increases with increasing of the JE concentration. The inhibitor efficiencies determined by weight loss, Tafel polarisation and EIS methods are in reasonable agreement. Based on the polarisation results, the investigated junipers extract can be classified as mixed inhibitor. The calculated structural parameters show increase of the obtained R_{ct} values and decrease of the capacitance, C_{dl} , with JE concentration increase. It is suggested to attribute this to the increase of the thickness of the adsorption layer at steel surface. The adsorption model obeys to the Langmuir adsorption isotherm. The adsorption process is a spontaneous and exothermic process.

ACKNOWLEDGEMENTS

Prof S. S. Deyab, Prof B. Hammouti and Prof R. Salghi extend their appreciation to the Deanship of Scientific Research at King Saud University for funding the work through the research group project No. RGP-VPP-089.

References

1. S. Ramesh, S. Rajeswari, S. Maruthamuthu, *Mater. Lett.* 57 (2003) 4547.
2. H. Zarrok, H. Oudda, A. Zarrouk, R. Salghi, B. Hammouti, M. Bouachrine, *Der Pharma Chemica*. 3 (2011) 576.
3. M. Mihit, K. Laarej, H. Abou El Makarim, L. Bazzi, R. Salghi, B. Hammouti, *Arabian J. Chem.* 3 (2010) 55.
4. M. Mihit, L. Bazzi, R. Salghi, B. Hammouti, S. El Issami, E. Ait Addi, *I. S. J. A. E. E.* 62 (2008) 173.
5. K. Barouni, L. Bazzi, R. Salghi, M. Mihit, B. Hammouti, A. Albourine, S. El Issami, *Mater. Lett.* 62 (2008) 3325.
6. S. El Issami, L. Bazzi, M. Mihit, B. Hammouti, S. Kertit, E. Ait Addi, R. Salghi, *Pigment & Resin. Tech.* 36 (2007) 161.
7. M. Mihit, R. Salghi, S. El Issami, L. Bazzi, B. Hammouti, El. Ait Addi, S. Kertit, *Pigment & Resin. Tech.* 35 (2006) 151.
8. M. Mihit, S. El Issami, M. Bouklah, L. Bazzi, B. Hammouti, E. Ait Addi, R. Salghi, S. Kertit, *Applied. Surf. Sci.* 252 (2006) 2389.
9. S. El Issami, L. Bazzi, M. Mihit, M. Hilali, R. Salghi, El. Ait Addi, *J. Phys. IV.* 123 (2005) 307.
10. S. El Issami, L. Bazzi, M. Hilali, R. Salghi, S. Kertit, *Ann. Chim. Sci. Mat.* 27 (2002) 63.
11. R. Salghi, L. Bazzi, B. Hammouti, S. Kertit, *Bull. of Electrochem.* 16 (2000) 272.
12. B. Hammouti, R. Salghi, S. Kertit, *J. Electrochem Soc. India.* 47 (1998) 31.
13. D. Ben Hmamou, R. Salghi, Lh. Bazzi, B. Hammouti, S.S. Al-Deyab, L. Bammou, L. Bazzi, A. Bouyanzer, *Int. J. Electrochem.Sci.* 7 (2012) 1303.
14. L. Afia, R. Salghi, L. Bammou. El. Bazzi, B. Hammouti, L. Bazzi, A. Bouyanzer, *Journal Saudia Chemistry Science.* 2066/10.1016/j.jscs.2011.05.008, (2012).
15. L. Afia, R. Salghi, El. Bazzi, L. Bazzi, M. Errami, O. Jbara, S. S Al-Deyab, B Hammouti, *Int. J. Electrochem. Sci.* 6 (2011) 5918.
16. L. Afia, R. Salghi, L. Bammou, Lh. Bazzi, B. Hammouti, L. Bazzi, *Acta Metall. Sin.* 25 (2012) 10.
17. L. Afia, R. Salghi, El. Bazzi, A. Zarrouk, B. Hammouti, M. Bouri, H. Zarrok, L. Bazzi, L. Bammou, *Res Chem Intermed* (2012) DOI 10.1007/s11164-012-0496-y.

18. N. Lahhit, A. Bouyanzer, J. M. Desjobert, B. Hammouti, R. Salghi, J. Costa, C. Jama, F. Bentiss, L. Majidi, *Port. Electrochim. Acta.* 29 (2011) 127.
19. A. Chetouani, B. Hammouti, M. Benkaddour, *Resin & Pigment Technol.* 33 (2004) 26.
20. E. El Ouariachi, J. Paolini, M. Bouklah, A. Elidrissi, A. Bouyanzer, B. Hammouti, J-M Desjobert, J. Costa, *Acta Metall. Sin.* 23 (2010) 13.
21. M. Bendahou, M. Benabdallah, B. Hammouti, *Pigm. Res. Techn.* 35 (2006) 95.
22. A Bouyanzer, B. Hammouti, *Bull. Electrochem.* 20 (2004) 63.
23. L. Bammou, B. Chebli, R. Salghi, L. Bazzi, B. Hammouti, M. Mihit, H. El Idrissi, *Green Chem. Lett. Rev.* 3 (2010) 173.
24. B. Zerga, M. Sfaira, Z. Rais, M. Ebn Touhami, M. Taleb, B. Hammouti, B. Imelouane, A. Elbachiri, *Materiaux et Technique.* 97 (2009) 297.
25. A. Bouyanzer, B. Hammouti, *Pigm. Resin & Techn.* 33 (2004) 287.
26. A. Bouyanzer, B. Hammouti, L. Majidi, *Mater. Lett.* 60 (2006) 2840.
27. L. Majidi, Z. Faska, M. Znini, S. Kharchouf, A. Bouyanzer, B. Hammouti *J. Mater. Environ. Sci.* 1 (2010) 219.
28. L. Bammou, M. Mihit, R. Salghi, L. Bazzi, A. Bouyanzer, B. Hammouti, *Int. J. Electrochem. Sci.* 6 (2011) 1454.
29. O. Ouachikh, A. Bouyanzer, M. Bouklah, J-M. Desjobert, J. Costa, B. Hammouti, L. Majidi, *Surf. Rev. Lett.* 16 (2009) 49.
30. M. Ajmal, A. S. Mideen, M. A Quraishi, *Corros. Sci.* 36 (1994) 79.
31. M. Behpour, S.M. Ghoreishi, M.K. Kashani, N. Soltani, *Mater. Corros.* 60 (2009) 895.
32. W. Wang, Y. Ding, D. M. Xing, J. P. Wang, L. J. J. Du, *Chinese. Mat. Med.* 31 (2006) 1242.
33. C. Ma, S. Xiao, Z. Li, W. Wang, L. Du, *J. Chromatogr A.* 1165 (2007) 39.
34. J.O'M. Bochriss., A. K. N. Reddy, *Modern Electrochemistry*, Plenum Press, New York, 2 (1977) 1267.
35. N. M. Guan, L. Xueming, L. Fei, *Mater. Chem. Phys.* 86 (2004) 59.
36. N. Soltani, M. Behpour, S. M. Ghoreishi, H. Naeimi, *Corros. Sci.* 52 (2010) 1351.
37. M. K. Gomma, M. H. Wahdan, *Mater. Chem. Phys.* 39 (1995) 209.
38. E. Kamis, *Corrosion.* 46 (1990) 478.
39. S. S. Adb El-Rehim, A. Magdy, M. Ibrahim, F. Khaled, *J. Appl. Electrochem.* 29 (1999) 599.
40. Mc Cafferty, E., in : H. Leidheiser Jr. (Ed.) *Corros Control by Coating*, Science press, Princeton (1979) 279.
41. G. Q. Uartarone, G. Moretti, A. Tassan, A. Zingales, *Werkst. Corros.* 45 (1994).
42. S. S. Abd El-Rehim, M. A. M. Ibrahim, K. F. Khaled, *J. Appl. Electrochem.* 29 (1999) 593.
43. M. Bouklah, N. Benchat, A. Aouniti, B. Hammouti, M. Benkaddour, M. Lagrenee, H. Vezin, F. Bentiss, *Prog. Org. Coat.* 51 (2004) 118.
44. M.S. Morad, A.M. K. El-Dean, *Corros. Sci.* 48 (2006) 3398.
45. K. Tebbji, B. Hammouti, H. Oudda, A. Ramdani, M. Benkadour, *Appl. Surf. Sci.* 252 (2005) 1378.
46. A. Yurt, A. Balaban, S. Ustun Kandemir, G. Bereket, B. Erk, *Mater. Chem. Phys.* 85 (2004) 420.
47. H. H. Hassan, E. Abdelghani, M. A. Amin, *Electrochim. Acta.* 52 (2007) 6359.
48. F. Bentiss, M Bouanis, B. Mernari, M. Traisnel, H. Vezin, M. Lagrenee, *Appl. Surf. Sci.* 253 (2007) 3696.
49. F. Bentiss, F. Gassama, D. Barbry, L. Gengembre, H. Vezin, M. Lagrenee, M. Traisnel, *Appl. Surf. Sci.* 252 (2006) 2684.
50. T. Tsuru, S. Haruyama, B., J. Gijutsu, *Soc. Corros. Eng.* 27 (1978) 573.
51. J.C. Da Rocha, J.A.C.P. Gomes, E. D'Elia, *Corros. Sci.* 52 (2010) 2341.
52. S.A. Umoren, I. B. Obot, N.O. Obi-Egbedi, *J. Mater. Sci.* 44 (2009) 274.